Establishing Platoons of Bidirectional Cooperative Vehicles with Engine Limits and Uncertain Dynamics

Baldi, Simone; Liu, Di; Jain, Vishrut; Yu, Wenwu

DOI
10.1109/TITS.2020.2973799

Publication date
2021

Document Version
Accepted author manuscript

Published in
IEEE Transactions on Intelligent Transportation Systems

Citation (APA)
Baldi, S., Liu, D., Jain, V., & Yu, W. (2021). Establishing Platoons of Bidirectional Cooperative Vehicles with Engine Limits and Uncertain Dynamics. *IEEE Transactions on Intelligent Transportation Systems*, *22*(5), 2679-2691. https://doi.org/10.1109/TITS.2020.2973799

Establishing platoons of bidirectional cooperative vehicles with engine limits and uncertain dynamics

Simone Baldi *Senior Member, IEEE*, Di Liu, Vishrut Jain, and Wenwu Yu *Senior Member, IEEE*

***Abstract*—In adaptive platooning strategies proposed in literature to handle uncertain and nonidentical uncertain vehicle dynamics (uncertain heterogeneous platoons) two aspects requiring proper design are neglected: *bidirectional interaction among vehicles* which might lead to loss of string stability, and *engine saturation constraints* which might lead to loss of cohesiveness. This work proposes a novel adaptive platooning strategy handling these two crucial aspects. Specifically, bidirectional interaction is handled by designing bidirectional reference dynamics with proven string stability properties, to which the uncertain heterogeneous platoon should homogenize; engine constraints are handled via a proposed a mechanism that makes such reference dynamics 'not too demanding', by properly saturating their action. The saturation action will allow all vehicles in the platoon to not hit their engine limits, preserving cohesiveness. Simulations are conducted to validate the theoretical analysis and show the effectiveness of the method in retaining cohesiveness of the platoon.**

Keywords: Cooperative adaptive cruise control, engine constraints, bidirectional communication, heterogeneous platoon.

I. Introduction

COOPERATIVE Adaptive Cruise Control (CACC), also referred to as platooning, is a way of grouping vehicles into platoons with a defined intervehicle spacing policy by using vehicle-to-vehicle wireless communication in addition to on-board sensors [1], [2]. After initial studies on homogeneous platoons [3], [4], it was soon recognized that several heterogeneities might influence the platooning effectiveness: networked-induced delays and packet losses have been well studied in literature as they generate some level of heterogeneity in wireless CACC communication [5]–[7]. Methods used to achieve platooning over unreliable communication include observers [8]–[10] or switched CACC strategies [11], [12].

This work was partly supported by the Fundamental Research Funds for the Central Universities grant no. 4007019109 (RECON-STRUCT), the special guiding funds 'double first-class' grant no. 4007019201, the China Scholarship Council (CSC) grant no. 201906090146, the Natural Science Foundation of China grant No. 61673107, the Ten Thousand Talent Program for Young Talents grant No. W2070082, the General joint fund of the equipment advance research program of Ministry of Education grant No. 6141A020223, the Jiangsu Provincial Key Lab of Networked Collective Intelligence grant No. BM2017002. (The first two authors equally contributed to this work.
Corresponding authors: Wenwu Yu and Simone Baldi)

S. Baldi is with School of Mathematics, Southeast University, Nanjing 210096, China, and also with Delft Center for Systems and Control, Delft University of Technology, 2628 CD, The Netherlands (e-mail: s.baldi@tudelft.nl)

D. Liu is with the School of Cyber Science and Engineering, Southeast University, Nanjing 210096, China and also with the Bernoulli Institute for Mathematics, Computer Science and Artificial Intelligence, University of Groningen, Groningen 9747AG, Netherlands (e-mail: di.liu@rug.nl)

V. Jain is with Delft Center for Systems and Control, Delft University of Technology, 2628 CD Delft, The Netherlands (email: v.jain-1@tudelft.nl).

W. Yu is with the School of Cyber Science and Engineering, Southeast University, Nanjing 210096, China, and also with the School of Mathematics, Southeast University, Nanjing 210096, China (e-mail: wwyu@seu.edu.cn)

However, a more substantial level of heterogeneity arises from the vehicle dynamics [13]: notably, cohesiveness of a platoon of nonidentical (heterogeneous) vehicles can be lost in the presence of engine saturating limits (e.g. a family car can lose cohesiveness in a platoon with sport cars). As opposed to standard unidirectional look-ahead interaction (where each vehicle adjusts the spacing with the front vehicle only), the use of bidirectional interaction (adjusting the spacing with both the front and the rear vehicle) was proposed to improve cohesiveness [14]. Unfortunately, bidirectionality creates the challenge of defining bidirectional string stability [15], [16] (string stability refers to the attenuation of disturbances as they propagate through the platoon [17]). This challenge makes the use of bidirectionality in CACC an open question: in fact, all forthcoming cited works refer to unidirectional platooning.

A pioneering work considering the fundamental control limitations in platoons was [18]; [19] also studied the limitations of platoons subject to saturation. Both works (and recent ones, [20] on homogeneous vehicles with actuator faults, [21] on homogeneous platoons with velocity constraints, [22] on low-gain control, [23] on antiwindup, [24] on car-following interaction) come to the same conclusion: loss of cohesiveness can be systematically eliminated only at the price of losing performance so as to prevent engine saturation. Unfortunately, these works on saturation do not focus on heterogeneous vehicle dynamics, an important source of heterogeneity and uncertainty. Recently, CACC strategies were proposed to address vehicle heterogeneity by adapting the control gains [25]–[27]. Such strategies define homogeneous reference dynamics that the heterogenous platoon should match. Distributed matching conditions define the control gains to match the reference dynamics [28]: with uncertain vehicle dynamics, such matching gains should be learned via appropriate adaptive laws [29]. The learning mechanism makes these strategies intrinsically nonlinear, and thus possibly more flexible than fixed-gain or linear CACC strategies.

Despite the progress in the CACC field[1], the research in this work stems from the following open questions: is it possible to improve platoon cohesiveness adaptively when the engine dynamics of the vehicles are uncertain and subject to saturation? Can the adaptation law benefit from the presence of bidirectional communication? The main contribution of this work is enhancing the adaptive platooning methodology by giving a positive answer to these questions.

As a first answer/contribution, we design bidirectional reference dynamics to which the heterogeneous platoon should

[1]The interested reader might consult recently published advances in IEEE ITS Special Issue on the 2016 Grand Cooperative Driving Challenge [30]–[33]

adaptively homogenize, and whose string stability properties are shown via appropriate criteria. As a second answer/contribution, we propose a mechanism that makes the reference dynamics 'not too demanding', by applying a properly designed saturation action that prevents all vehicles from hitting their engine bounds. This is in line with the studies [18], [19], i.e. saturation can be eliminated only at the price of losing performance. As even the most recent literature on platooning focuses on longitudinal dynamics (lateral string stability and nonholonomic constraints arising from lateral dynamics are unsolved challenges up to now [32], [34]–[38]), in this work we will also consider longitudinal dynamics.

The paper is organized as follows. In Section II, a CACC platoon with bidirectional interaction and string stability properties is presented. Engine saturation is introduced in Section III, together with the proposed adaptive mechanism. Simulation results are presented in Section IV.

II. CACC System Structure

Consider the platoon in Fig. 1, where v_i and d_i represent the velocity (m/s) of vehicle i, and the spacing (m) between vehicle i and its preceding vehicle. As Fig. 1, highlights, let us considers a bidirectional communication with preceding and succeeding vehicle, an extension of the unidirectional look-ahead communication with preceding vehicle [3].

A constant time headway policy regulates the spacing between vehicles, implemented by defining the look-ahead desired spacing $d_{des,f,i}$ and look-back desired spacing $d_{des,b,i}$:

$$d_{des,f,i}(t) = r_i + hv_i(t)$$
$$d_{des,b,i}(t) = r_i + hv_{i+1}(t) \ , \ i \in S_M$$

where r_i is the standstill distance (m), h the time headway (s), and $S_M = \{i \in \mathbb{N} | \ 1 \le i \le M\}$, being M the number of vehicles and $i = 0$ reserved for the leading vehicle.

With bidirectionality, errors in both the look-ahead and look-back direction are considered, the look-ahead error being

$$\begin{aligned} e_{f,i}(t) &= d_{i-1,i}(t) - d_{des,f,i}(t) \\ &= (q_{i-1}(t) - q_i(t) - L_i) - (r_i + hv_i(t)) \end{aligned} \tag{1}$$

and the look-back error being

$$\begin{aligned} e_{b,i}(t) &= -(d_{i,i+1}(t) - d_{des,b,i}(t)) \\ &= -((q_i(t) - q_{i+1}(t) - L_{i+1}) - (r_i + hv_{i+1}(t))) \end{aligned} \tag{2}$$

with q_i and L_i representing vehicle i's rear-bumper position (m) and length (m), and $d_{i-1,i}$ and $d_{i,i+1}$ representing the intervehicle distances. The sign convention for the look-back error is chosen to be opposite to the look-ahead error (as the errors point in different directions). Finally, the total spacing error is taken as the convex combination of $e_{f,i}$ and $e_{b,i}$

$$e_i(t) = c_1 e_{f,i}(t) + c_2 e_{b,i}(t), \qquad 1 \le i < M \tag{3}$$

with $c_1 \in (0, 1]$ and $c_2 = 1 - c_1$. Note that for $c_1 = 1$ and $c_2 = 0$ one would have the standard CACC unidirectional situation in which only the look-ahead spacing error is considered. For $c_1 = c_2 = 0.5$ one would have a bidirectional situation in which look-ahead and look-back errors are equally weighted.

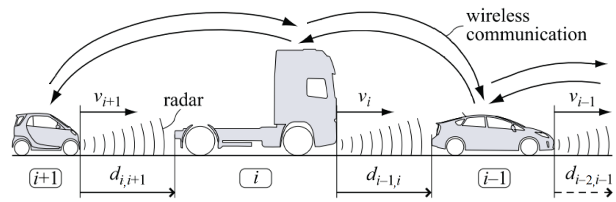

Fig. 1: CACC-equipped heterogeneous vehicle platoon with bidirectional communication (edited from [36]).

As the leading and the last vehicle can only measure look-back and look-ahead error respectively, their error is simply

$$e_0(t) = e_{b,0}(t) = q_1(t) - q_0(t) + L_1 + r + hv_1(t)$$
$$e_M(t) = e_{f,M}(t) = q_{M-1}(t) - q_M(t) - L_M - r - hv_M(t).$$

The control objective is to regulate e_i to zero $\forall i \in S_M \cup \{0\}$, while ensuring string stability of the platoon. Upon regulation of e_i to zero, the platoon is said to be *cohesive*.

Remark 1: The notion of cohesiveness is intrinsic to the spacing policy: while for a constant distance policy the relative distance is a good measure of cohesiveness, the best measure of cohesiveness for a constant time headway policy is the spacing error (3)*, as the relative distance is velocity dependent. In both constant distance and constant time headway policies, the relative velocities, to be regulated to zero to keep the platoon cohesive, are another good measure of cohesiveness.*

The following model is standard [3] to represent the vehicles in the platoon

$$\begin{pmatrix} \dot{d}_i \\ \dot{v}_i \\ \dot{a}_i \end{pmatrix} = \begin{pmatrix} v_{i-1} - v_i \\ a_i \\ -\frac{1}{\tau_i} a_i + \frac{1}{\tau_i} u_i \end{pmatrix} \ , \ i \in S_M \cup \{0\} \tag{4}$$

with a_i and u_i being the acceleration (m/s^2) and input (m/s^2), and τ_i (s) being the engine time constant of the i^{th} vehicle.

In the following we address three basic concepts for a homogeneous platoon with identical τ_i: design a baseline CACC protocol (Sect. II.A); define and analyze bidirectional string stability (Sect. II.B); introduce uncertainty in the vehicle dynamics (Sect. II.C). Let us focus on the unsaturated case, while saturation will be covered in Sect. III.

A. The CACC control structure

The control action can be designed by formulating the error dynamics. Define the error states as

$$\begin{pmatrix} e_{1,i} \\ e_{2,i} \\ e_{3,i} \end{pmatrix} = \begin{pmatrix} e_i \\ \dot{e}_i \\ \ddot{e}_i \end{pmatrix} \ , \ 0 \le i \le M. \tag{5}$$

State-of-the-art CACC protocols design the control action assuming identical τ_i (baseline homogeneous condition) [3], so that the baseline control input (indicated with the subscript *bl*) can be derived from the dynamics of $e_{3,i}$, via (3) and (4)

$$\begin{aligned} \dot{e}_{3,i} = &- \frac{1}{\tau_i} e_{3,i} - \frac{1}{\tau_i} p_i \\ &+ \frac{c_1}{\tau_i} u_{i-1,bl} + \frac{c_2}{\tau_i} u_{i+1,bl} + \frac{hc_2}{\tau_i} \dot{u}_{i+1,bl} \end{aligned} \tag{6}$$

with $p_i = u_{i,bl} + hc_1\dot{u}_{i,bl}$. From (6) it is clear that p_i should stabilize the error dynamics (5) while compensating for the terms $u_{i-1,bl}$, $u_{i+1,bl}$ and $\dot{u}_{i+1,bl}$. Hence, define p_i as

$$p_i = (k_p \; k_d \; k_{dd}) \begin{pmatrix} e_{1,i} \\ e_{2,i} \\ e_{3,i} \end{pmatrix} + c_1 u_{i-1,bl} + c_2 u_{i+1,bl} + hc_2 \dot{u}_{i+1,bl} \tag{7}$$

with k_p, k_d and k_{dd} being gains to be designed in order to have stability/string stability specifications. The feedforward terms $u_{i-1,bl}$, $u_{i+1,bl}$ and $\dot{u}_{i+1,bl}$ can be obtained via wireless communication with the preceding and succeeding vehicle [3].

From (7) the controller dynamics is given by

$$\dot{u}_{i,bl} = -\frac{1}{hc_1}u_{i,bl} + \frac{1}{hc_1}(k_p e_{1,i} + k_d e_{2,i} + k_{dd} e_{3,i}) + \frac{1}{h}u_{i-1,bl} + \frac{c_2}{hc_1}u_{i+1,bl} + \frac{c_2}{c_1}\dot{u}_{i+1,bl}. \tag{8}$$

It is well known in literature that k_{dd} can be set to be zero to avoid feedback from the relative acceleration, which is very difficult to get in practice [39]. This results in

$$\begin{pmatrix} \dot{e}_{1,i} \\ \dot{e}_{2,i} \\ \dot{e}_{3,i} \\ \dot{u}_{i,bl} \end{pmatrix} = \begin{pmatrix} 0 & 1 & 0 & 0 \\ 0 & 0 & 1 & 0 \\ -\frac{k_p}{\tau_i} & -\frac{k_d}{\tau_i} & -\frac{1}{\tau_i} & 0 \\ \frac{k_p}{hc_1} & \frac{k_d}{hc_1} & 0 & -\frac{1}{hc_1} \end{pmatrix} \begin{pmatrix} e_{1,i} \\ e_{2,i} \\ e_{3,i} \\ u_{i,bl} \end{pmatrix} + \begin{pmatrix} 0 & 0 & 0 \\ 0 & 0 & 0 \\ 0 & 0 & 0 \\ \frac{1}{h} & \frac{c_2}{hc_1} & \frac{c_2}{c_1} \end{pmatrix} \begin{pmatrix} u_{i-1,bl} \\ u_{i+1,bl} \\ \dot{u}_{i+1,bl} \end{pmatrix} \; \forall i \in S_M \setminus \{M\}. \tag{9}$$

If the errors are written in terms of velocity and acceleration, (9) can be equivalently written, $\forall i \in S_M \setminus \{M\}$, as

$$\begin{pmatrix} \dot{e}_i \\ \dot{v}_i \\ \dot{a}_i \\ \dot{u}_{i,bl} \end{pmatrix} = \begin{pmatrix} 0 & -1 & -hc_1 & 0 \\ 0 & 0 & 1 & 0 \\ 0 & 0 & -\frac{1}{\tau_i} & \frac{1}{\tau_i} \\ \frac{k_p}{hc_1} & -\frac{k_d}{hc_1} & -k_d & -\frac{1}{hc_1} \end{pmatrix} \begin{pmatrix} e_i \\ v_i \\ a_i \\ u_{i,bl} \end{pmatrix} + \begin{pmatrix} c_1 & c_2 & hc_2 & 0 & 0 & 0 \\ 0 & 0 & 0 & 0 & 0 & 0 \\ 0 & 0 & 0 & 0 & 0 & 0 \\ \frac{k_d}{h} & \frac{k_d c_2}{hc_1} & \frac{k_d c_2}{c_1} & \frac{1}{h} & \frac{c_2}{hc_1} & \frac{c_2}{c_1} \end{pmatrix} \begin{pmatrix} v_{i-1} \\ v_{i+1} \\ a_{i+1} \\ u_{i-1,bl} \\ u_{i+1,bl} \\ \dot{u}_{i+1,bl} \end{pmatrix} \tag{10}$$

which represents the dynamics of a vehicle equipped with baseline CACC protocol. Notice that (9) (or (10)) are valid for $i \in S_M \setminus \{M\}$, i.e. only for those vehicles with both a front and a rear vehicle. The leading vehicles and the last vehicle obey slightly different dynamics, as clarified hereafter.

B. Analysis of bidirectional string stability

String stability refers to the capability of CACC to attenuate exogenous inputs (e.g. leader input) as they propagate through the platoon. To analyze if a platoon is string stable we need to derive the corresponding interconnected dynamics. Available CACC string stability criteria are based on homogeneity of the vehicles: without loss of generality we consider homogeneity with respect to the leading vehicle, i.e., $\tau_i = \tau_0, \forall i$. To proceed with the analysis, we will write the interconnections among vehicles in a compact way, by defining the state

$$t_i = c_1 u_{i,bl} - c_2 u_{i+1,bl}, \quad 0 \le i < M-1$$
$$t_M = c_1 u_{M,bl}, \qquad i = M. \tag{11}$$

It can be noticed that

$$c_1 u_{i,bl} = t_i + \frac{c_2}{c_1}t_{i+1} + \left(\frac{c_2}{c_1}\right)^2 t_{i+2} + \ldots + \left(\frac{c_2}{c_1}\right)^{M-i} t_M. \tag{12}$$

After manipulating (10) via (12) we obtain, $i \in S_M \setminus \{M\}$

$$\underbrace{\begin{pmatrix} \dot{e}_i \\ \dot{v}_i \\ \dot{a}_i \\ \dot{t}_i \end{pmatrix}}_{\dot{\chi}_i} = \underbrace{\begin{pmatrix} 0 & -1 & -hc_1 & 0 \\ 0 & 0 & 1 & 0 \\ 0 & 0 & -\frac{1}{\tau_0} & \frac{1}{\tau_0 c_1} \\ \frac{k_p}{h} & -\frac{k_d}{h} & -k_d c_1 & -\frac{1}{h} \end{pmatrix}}_{A_0} \underbrace{\begin{pmatrix} e_i \\ v_i \\ a_i \\ t_i \end{pmatrix}}_{\chi_i} + \underbrace{\begin{pmatrix} 0 & c_1 & 0 & 0 \\ 0 & 0 & 0 & 0 \\ 0 & 0 & 0 & 0 \\ 0 & \frac{k_d c_1}{h} & 0 & \frac{1}{h} \end{pmatrix}}_{A_{-1}} \underbrace{\begin{pmatrix} e_{i-1} \\ v_{i-1} \\ a_{i-1} \\ t_{i-1} \end{pmatrix}}_{\chi_{i-1}} + \underbrace{\begin{pmatrix} 0 & c_2 & hc_2 & 0 \\ 0 & 0 & 0 & 0 \\ 0 & 0 & 0 & \frac{c_2}{\tau_0 {c_1}^2} \\ 0 & \frac{k_d c_2}{h} & k_d c_2 & 0 \end{pmatrix}}_{A_1} \underbrace{\begin{pmatrix} e_{i+1} \\ v_{i+1} \\ a_{i+1} \\ t_{i+1} \end{pmatrix}}_{\chi_{i+1}} + \cdots + \underbrace{\begin{pmatrix} 0 & 0 & 0 & 0 \\ 0 & 0 & 0 & 0 \\ 0 & 0 & 0 & \frac{{c_2}^{M-i}}{\tau_0 {c_1}^{M+1-i}} \\ 0 & 0 & 0 & 0 \end{pmatrix}}_{A_{M-i}} \underbrace{\begin{pmatrix} e_M \\ v_M \\ a_M \\ t_M \end{pmatrix}}_{\chi_M}. \tag{13}$$

which holds for all vehicles in the platoon, excluding the leading and the last vehicle. In fact, as the last vehicle has no following vehicles, we define the unidirectional CACC control

$$h\dot{u}_{M,bl} = -u_{M,bl} + (k_p e_{1,M} + k_d e_{2,M}) + u_{M-1,bl} \tag{14}$$

which becomes, in terms of t_M,

$$h\dot{t}_M = \frac{c_2 - c_1}{c_1}t_M + c_1(k_p e_{1,M} + k_d e_{2,M}) + t_{M-1}. \tag{15}$$

Hence the dynamics of the last vehicle can be described by

$$\dot{\chi}_M = \underbrace{\begin{pmatrix} 0 & -1 & -h & 0 \\ 0 & 0 & 1 & 0 \\ 0 & 0 & -\frac{1}{\tau_0} & \frac{1}{\tau_0 c_1} \\ \frac{k_p c_1}{h} & -\frac{k_d c_1}{h} & -k_d c_1 & \frac{c_2 - c_1}{hc_1} \end{pmatrix}}_{E_0} \chi_M + \underbrace{\begin{pmatrix} 0 & 1 & 0 & 0 \\ 0 & 0 & 0 & 0 \\ 0 & 0 & 0 & 0 \\ 0 & \frac{k_d c_1}{h} & 0 & \frac{1}{h} \end{pmatrix}}_{E_{-1}} \chi_{M-1}. \tag{16}$$

On the other end, after using $t_0 = c_1 u_{0,bl} - c_2 u_{1,bl}$, the dynamics of the leading vehicle become

$$\dot{\chi}_0 = \begin{pmatrix} 0 & -1 & 0 & 0 \\ 0 & 0 & 1 & 0 \\ 0 & 0 & -\frac{1}{\tau_0} & 0 \\ \frac{k_p c_2}{h} & -\frac{k_d c_2}{h} & 0 & -\frac{1}{h} - \frac{c_2}{hc_1} \end{pmatrix} \chi_0 \qquad (17)$$
$$+ \begin{pmatrix} 0 & 1 & h & 0 \\ 0 & 0 & 0 & 0 \\ 0 & 0 & 0 & 0 \\ 0 & \frac{k_d c_2}{h} & k_d c_2 & 0 \end{pmatrix} \chi_1 + \begin{pmatrix} 0 \\ 0 \\ \frac{1}{\tau_0} \\ -\frac{c_2}{h} \end{pmatrix} u_{0,bl} + \begin{pmatrix} 0 \\ 0 \\ 0 \\ \frac{c_1}{h} \end{pmatrix} u_r.$$

The leader vehicle is the only vehicle that can set the platoon acceleration u_r as the exogenous input. That is, (17) has been derived by imposing the leader control action as

$$hc_1 \dot{u}_{0,bl} = -u_{0,bl} + c_2(k_p e_{1,0} + k_d e_{2,0}) + u_r + c_2 u_{1,bl} + hc_2 \dot{u}_{1,bl} \qquad (18)$$

which becomes, in terms of t_0,

$$h\dot{t}_0 = \left(-1 - \frac{c_2}{c_1}\right) t_0 + c_2(k_p e_{1,0} + k_d e_{2,0}) - \left(\frac{c_2}{c_1}\right)^2 t_1$$
$$- \left(\frac{c_2}{c_1}\right)^3 t_2 - \ldots - \left(\frac{c_2}{c_1}\right)^{M+1} t_M + u_r. \qquad (19)$$

The importance of (13), (16) and (17) is to allow checking how the effect of the exogenous input u_r propagates throughout a bidirectional platoon. To analyze such effect, we write $u_{0,bl}$ in (17) as a function of the states of the vehicles via (12). Hence, (17) becomes

$$\begin{pmatrix} \dot{e}_0 \\ \dot{v}_0 \\ \dot{a}_0 \\ \dot{t}_0 \end{pmatrix} = \underbrace{\begin{pmatrix} 0 & -1 & 0 & 0 \\ 0 & 0 & 1 & 0 \\ 0 & 0 & -\frac{1}{\tau_0} & \frac{1}{\tau_0 c_1} \\ \frac{k_p c_2}{h} & -\frac{k_d c_2}{h} & 0 & -\frac{1}{h} - \frac{c_2}{hc_1} \end{pmatrix}}_{F_0} \begin{pmatrix} e_0 \\ v_0 \\ a_0 \\ t_0 \end{pmatrix} \qquad (20)$$
$$+ \underbrace{\begin{pmatrix} 0 & 1 & h & 0 \\ 0 & 0 & 0 & 0 \\ 0 & 0 & 0 & \frac{1}{\tau_0 c_1}\frac{c_2}{c_1} \\ 0 & \frac{k_d c_2}{h} & k_d c_2 & -\frac{1}{h}(\frac{c_2}{c_1})^2 \end{pmatrix}}_{F_1} \begin{pmatrix} e_1 \\ v_1 \\ a_1 \\ t_1 \end{pmatrix}$$
$$+ \underbrace{\begin{pmatrix} 0 & 0 & 0 & 0 \\ 0 & 0 & 0 & 0 \\ 0 & 0 & 0 & \frac{1}{\tau_0 c_1}(\frac{c_2}{c_1})^2 \\ 0 & 0 & 0 & -\frac{1}{h}(\frac{c_2}{c_1})^3 \end{pmatrix}}_{F_2} \begin{pmatrix} e_2 \\ v_2 \\ a_2 \\ t_2 \end{pmatrix} + \ldots$$
$$+ \underbrace{\begin{pmatrix} 0 & 0 & 0 & 0 \\ 0 & 0 & 0 & 0 \\ 0 & 0 & 0 & \frac{1}{\tau_0 c_1}(\frac{c_2}{c_1})^M \\ 0 & 0 & 0 & -\frac{1}{h}(\frac{c_2}{c_1})^{M+1} \end{pmatrix}}_{F_M} \begin{pmatrix} e_M \\ v_M \\ a_M \\ t_M \end{pmatrix} + \underbrace{\begin{pmatrix} 0 \\ 0 \\ 0 \\ \frac{1}{h} \end{pmatrix}}_{B_0} u_r.$$

The coefficients $\frac{c_2}{c_1}$, $\left(\frac{c_2}{c_1}\right)^2$, ..., $\left(\frac{c_2}{c_1}\right)^M$ arise from the bidirectional interconnection (12). To complete the analysis, let us define the platoon state $\chi_{pl} = (\chi_0^T \ \chi_1^T \ \ldots \ \chi_M^T)^T$, the platoon output $y_{pl} = (a_0 \ a_1 \ \ldots \ a_M)^T$ and write (11)-(20) in the form

$$\dot{\chi}_{pl} = A_{pl}\chi_{pl} + B_{pl} u_r$$
$$y_{pl} = C_{pl}\chi_{pl} \qquad (21)$$

$$A_{pl} = \begin{pmatrix} F_0 & F_1 & F_2 & \ldots & F_{M-1} & F_M \\ A_{-1} & A_0 & A_1 & \ldots & A_{M-2} & A_{M-1} \\ 0 & A_{-1} & A_0 & \ldots & A_{M-3} & A_{M-2} \\ \vdots & \vdots & \vdots & \ddots & \vdots & \\ 0 & 0 & 0 & \ldots & E_{-1} & E_0 \end{pmatrix}$$
$$B_{pl} = \begin{pmatrix} B_0 \\ 0 \\ \vdots \\ 0 \end{pmatrix}, \ C_{pl} = \begin{pmatrix} C & 0 & \ldots & 0 \\ 0 & C & \ldots & 0 \\ \vdots & \vdots & \ddots & \vdots \\ 0 & 0 & \ldots & C \end{pmatrix}$$

and $C = (0 \ 0 \ 1 \ 0)$. Let us denote with $G_{i,r}(s)$, $i \in S_M \cup \{0\}$, the transfer functions from u_r to a_i, calculated from (21). The following notion of string stability is proposed:

***Definition** 1:* The platoon represented by (11)-(20) (or equivalently (21)) is string stable if $G_{i,r}(s)$ is stable and

$$|G_{i+1,r}(j\omega)| \leq |G_{i,r}(j\omega)|, \quad \forall\omega, 0 \leq i \leq M \qquad (22)$$

where $|\cdot|$ indicates the magnitude of the transfer function.

Remark 2: Similarly to [3], (22) *implies attenuation of exogenous effects throughout the platoon: however, the analysis* (11)-(20) *leading to* (21)-(22) *extends the approach in [3], as it is valid for both unidirectional and bidirectional cases.*

C. Engine heterogeneities

Having defined string stability for a bidirectional homogeneous platoon, let us see how to handle heterogeneity in τ_i, by representing it as the sum of two terms

$$\tau_i = \tau_0 + \Delta\tau_i \qquad (23)$$

where $\Delta\tau_i$ is a perturbation with respect to τ_0. Two approaches can be used to handle $\Delta\tau_i$, i.e. treating $\Delta\tau_i$ as known (robust control approach [20]–[23]) or as unknown (adaptive control approach [25]–[27]). With the intent of pursuing an adaptive approach, lets us use (23) in the third equation of (4)

$$\dot{a}_i = -\frac{1}{\tau_0}a_i + \frac{1}{\tau_0}\left[u_i + \Omega_i^*\phi_i\right], \ , \ \forall i \in S_M \qquad (24)$$

where $\Omega_i^* = -\frac{\Delta\tau_i}{\tau_i}$ is an unknown scalar, and $\phi_i = (u_i - a_i)$ is the known scalar regressor. Using (24) in (4), we get

$$\begin{pmatrix} \dot{e}_i \\ \dot{v}_i \\ \dot{a}_i \end{pmatrix} = \begin{pmatrix} 0 & -1 & -hc_1 \\ 0 & 0 & 1 \\ 0 & 0 & -\frac{1}{\tau_0} \end{pmatrix} \begin{pmatrix} e_i \\ v_i \\ a_i \end{pmatrix} + \begin{pmatrix} c_1 \\ 0 \\ 0 \end{pmatrix} v_{i-1}$$
$$+ \begin{pmatrix} c_2 & hc_2 \\ 0 & 0 \\ 0 & 0 \end{pmatrix} \begin{pmatrix} v_{i+1} \\ a_{i+1} \end{pmatrix} + \begin{pmatrix} 0 \\ 0 \\ \frac{1}{\tau_0} \end{pmatrix} \left[u_i + \Omega_i^*\phi_i\right]. \qquad (25)$$

Remark 3: As small delays are often modelled as first-order lag (see e.g. [40, Sect. 6.5]), the time constant τ_i can be thought to possibly include engine delay. Assuming τ_i to be unknown would then automatically include such delays. Robust adaptive control approaches as in [28] can also be adopted to handle delays and unmodelled dynamics.

III. Engine-constrained Control

Under the baseline conditions of identical vehicles ($\Omega_i^* = 0$), the following CACC control was derived in Sect. II

$$hc_1\dot{u}_{i,bl} = -u_{i,bl} + \xi_{i,bl}, \quad \forall i \in S_M \cup \{0\} \tag{26}$$

$$\xi_{i,bl} = \begin{cases} c_1 u_r + k_p e_0 + k_d \dot{e}_0 \\ \quad + c_2 u_{1,bl} + hc_2 \dot{u}_{1,bl} & i = 0. \\ k_p e_i + k_d \dot{e}_i + c_1 u_{i-1,bl} \\ \quad + c_2 u_{i+1,bl} + hc_2 \dot{u}_{i+1,bl} & i \in S_M \setminus \{M\} \\ k_p e_M + k_d \dot{e}_M + u_{M-1,bl} & i = M. \end{cases}$$

With the purpose of using the homogeneous condition as reference dynamics to which the heterogeneous platoon should converge, define $\forall i \in S_M \setminus \{M\}$ ($i = M$ omitted for brevity)

$$\begin{pmatrix} \dot{e}_{i,m} \\ \dot{v}_{i,m} \\ \dot{a}_{i,m} \\ \dot{u}_{i,m} \end{pmatrix} = \underbrace{\begin{pmatrix} 0 & -1 & -hc_1 & 0 \\ 0 & 0 & 1 & 0 \\ 0 & 0 & -\frac{1}{\tau_0} & \frac{1}{\tau_0} \\ \frac{k_p}{hc_1} & -\frac{k_d}{hc_1} & -k_d & -\frac{1}{hc_1} \end{pmatrix}}_{A_m} \underbrace{\begin{pmatrix} e_{i,m} \\ v_{i,m} \\ a_{i,m} \\ u_{i,m} \end{pmatrix}}_{x_{i,m}} + \underbrace{\begin{pmatrix} c_1 & c_2 & hc_2 & 0 & 0 & 0 \\ 0 & 0 & 0 & 0 & 0 & 0 \\ 0 & 0 & 0 & 0 & 0 & 0 \\ \frac{k_d}{h} & \frac{k_d c_2}{hc_1} & \frac{k_d c_2}{c_1} & \frac{1}{h} & \frac{c_2}{hc_1} & \frac{c_2}{c_1} \end{pmatrix}}_{B_w} \underbrace{\begin{pmatrix} v_{i-1} \\ v_{i+1} \\ a_{i+1} \\ u_{i-1,bl} \\ u_{i+1,bl} \\ \dot{u}_{i+1,bl} \end{pmatrix}}_{w_i} \tag{27}$$

where subscript m stands for model-reference, $x_{i,m}$ is the reference state and w_i contains variables coming from the actual vehicles in (10): consequently, (27) is in the form

$$\dot{x}_{i,m} = A_m x_{i,m} + B_w w_i, \forall i \in S_M. \tag{28}$$

Furthermore, the leading vehicle model becomes

$$\begin{pmatrix} \dot{e}_0 \\ \dot{v}_0 \\ \dot{a}_0 \\ \dot{u}_{0,bl} \end{pmatrix} = \underbrace{\begin{pmatrix} 0 & 0 & 0 & 0 \\ 0 & 0 & 1 & 0 \\ 0 & 0 & -\frac{1}{\tau_0} & \frac{1}{\tau_0} \\ \frac{k_p}{hc_1} & -\frac{k_d}{hc_1} & -k_d & -\frac{1}{hc_1} \end{pmatrix}}_{A_r} \underbrace{\begin{pmatrix} e_0 \\ v_0 \\ a_0 \\ u_{0,bl} \end{pmatrix}}_{x_0} + \begin{pmatrix} c_2 & hc_2 & 0 & 0 \\ 0 & 0 & 0 & 0 \\ 0 & 0 & 0 & 0 \\ \frac{k_d c_2}{hc_1} & \frac{k_d c_2}{c_1} & \frac{c_2}{hc_1} & \frac{c_2}{c_1} \end{pmatrix} \begin{pmatrix} v_1 \\ a_1 \\ u_{1,bl} \\ \dot{u}_{1,bl} \end{pmatrix} + \underbrace{\begin{pmatrix} 0 \\ 0 \\ 0 \\ \frac{1}{h} \end{pmatrix}}_{B_r} u_r. \tag{29}$$

Having defined the reference dynamics (29), two questions are now addressed: introduce adaptation in (26) to handle heterogeneities (23) (Sect. III.A); modify (26) and (29) to handle saturation constraints (Sect. III.B).

A. Adaptive CACC augmentation

The dynamics (28) can used as a reference model for the uncertain platoon's dynamics (25). With this scope in mind, we augment the baseline controller (26) with an adaptive term

$$u_i = u_{i,bl} + u_{i,ad} \tag{30}$$

where $u_{i,ad}$ is the adaptive augmentation controller (to be constructed). Replacing (30) into (25) results in

$$\begin{pmatrix} \dot{e}_i \\ \dot{v}_i \\ \dot{a}_i \\ \dot{u}_{i,bl} \end{pmatrix} = \begin{pmatrix} 0 & -1 & -hc_1 & 0 \\ 0 & 0 & 1 & 0 \\ 0 & 0 & -\frac{1}{\tau_0} & \frac{1}{\tau_0} \\ \frac{k_p}{hc_1} & -\frac{k_d}{hc_1} & -k_d & -\frac{1}{hc_1} \end{pmatrix} \underbrace{\begin{pmatrix} e_i \\ v_i \\ a_i \\ u_i \end{pmatrix}}_{x_i} + \begin{pmatrix} c_1 & c_2 & hc_2 & 0 & 0 & 0 \\ 0 & 0 & 0 & 0 & 0 & 0 \\ 0 & 0 & 0 & 0 & 0 & 0 \\ \frac{k_d}{h} & \frac{k_d c_2}{hc_1} & \frac{k_d c_2}{c_1} & \frac{1}{h} & \frac{c_2}{hc_1} & \frac{c_2}{c_1} \end{pmatrix} \begin{pmatrix} v_{i-1} \\ v_{i+1} \\ a_{i+1} \\ u_{i-1,bl} \\ u_{i+1,bl} \\ \dot{u}_{i+1,bl} \end{pmatrix} + \underbrace{\begin{pmatrix} 0 \\ 0 \\ \frac{1}{\tau_0} \\ 0 \end{pmatrix}}_{B_u} \left[u_{i,ad} + \Omega_i^* \phi_i\right], \quad \forall i \in S_M \tag{31}$$

Note that the leading vehicle's model is still as in (29). Define the adaptive augmentation control input to estimate and compensate for the unknown term $\Omega_i^* \phi_i$ as

$$u_{i,ad} = -\hat{\Omega}_i \phi_i \tag{32}$$

where $\hat{\Omega}_i$ is the estimate of Ω_i^*. Replacing (32) in (31) gives

$$\dot{x}_i = A_m x_i + B_w w_i - B_u (\underbrace{\hat{\Omega}_i - \Omega_i^*}_{\tilde{\Omega}_i})^T \phi_i \tag{33}$$

where $\tilde{\Omega}_i$ is the parameter estimation's error vector. Defining the state tracking error as $\tilde{x}_i = x_i - x_{i,m}$ we obtain the following state error dynamics

$$\dot{\tilde{x}}_i = A_m \tilde{x}_i + B_u \tilde{\Omega}_i \phi_i \tag{34}$$

Remark 4: Each vehicle can calculate $\tilde{x}_i$ by implementing a copy of the reference dynamics (27)*: then, the objective of each vehicle is to drive $\tilde{x}_i$ to zero. Upon convergence of $\tilde{x}_i$ to zero, the heterogeneous platoon converges to the behavior of a homogeneous platoon resulting from connecting the reference dynamics* (27) *in a platoon (Fig. 2).*

B. Saturated case

Let us now modify the reference dynamics (27) to handle saturation constraints: first, let us define $\xi_{i,m} = k_p e_i + k_d \dot{e}_i + c_1 u_{i-1,m} + c_2 u_{i+1,m} + hc_2 \dot{u}_{i+1,m}$ (similarly to (26)). Then

$$hc_1 \dot{u}_{i,m} = \begin{cases} 0 & \text{if } u_{i,m} = u_{max,m} \text{ and} \\ & \quad -u_{i,m} + \xi_{i,m} \geq 0 \\ -u_{i,m} + \xi_{i,m} & \text{if } u_{min,m} < u_{i,m} < u_{max,m} \\ & \quad \textbf{or } u_{i,m} = u_{max,m} \text{ and} \\ & \quad -u_{i,m} + \xi_{i,m} < 0 \\ & \quad \textbf{or } u_{i,m} = u_{min,m} \text{ and} \\ & \quad -u_{i,m} + \xi_{i,m} > 0 \\ 0 & \text{if } u_{i,m} = u_{min,m} \text{ and} \\ & \quad -u_{i,m} + \xi_{i,m} \leq 0 \end{cases} \tag{35}$$

where $u_{min,m}$ and $u_{max,m}$ are the saturation levels of the reference model to be designed. Such levels should be designed such that the vehicles in the platoon do not hit their saturation bounds, i.e. the reference model is not too demanding.

Remark 5: *Note that (35) provides an anti-windup action, as $\dot{u}_{i,m} = 0$ whenever the saturation bounds are hit. That is, $u_{i,m}$ stays at the saturation level ($u_{max,m}$ or $u_{min,m}$), and will immediately exit the saturation whenever $-u_{i,m} + \xi_{i,m} < 0$ or $-u_{i,m} + \xi_{i,m} > 0$.*

When saturation is hit, we find γ such that $-\gamma u_{i,m} + k_p e_i + k_d \dot{e}_i + c_1 u_{i-1,m} + c_2 u_{i+1,m} + hc_2 \dot{u}_{i+1,m} = 0$. This leads to the saturated dynamics, $\forall i \in S_M$

$$\begin{pmatrix}\dot e_{i,m}\\ \dot v_{i,m}\\ \dot a_{i,m}\\ \dot u_{i,m}\end{pmatrix} = \underbrace{\begin{pmatrix}0 & -1 & -hc_1 & 0\\ 0&0&1&0\\ 0&0&-\frac{1}{\tau_0}&\frac{1}{\tau_0}\\ \frac{k_p}{hc_1} & -\frac{k_d}{hc_1} & -k_d & -\frac{\gamma}{hc_1}\end{pmatrix}}_{A_m^\gamma}\underbrace{\begin{pmatrix}e_{i,m}\\v_{i,m}\\a_{i,m}\\u_{i,m}\end{pmatrix}}_{x_{i,m}} + \underbrace{\begin{pmatrix}c_1&c_2&hc_2&0&0&0\\0&0&0&0&0&0\\0&0&0&0&0&0\\ \frac{k_d}{h}&\frac{k_dc_2}{hc_1}&\frac{k_dc_2}{c_1}&\frac{1}{h}&\frac{c_2}{hc_1}&\frac{c_2}{c_1}\end{pmatrix}}_{B_w}\underbrace{\begin{pmatrix}v_{i-1}\\v_{i+1}\\a_{i+1}\\u_{bl,i-1}\\u_{bl,i+1}\\\dot u_{i+1}\end{pmatrix}}_{w_i} \tag{36}$$

Let us now design $u_{min,m}$ and $u_{max,m}$. We can prove that $u_{ad,i} \in [\bar{\Omega}(u_{i,min} - u_{i,max}), \bar{\Omega}(u_{i,max} - u_{i,min})]$, where $\bar{\Omega} = \max(|\Omega_{i,min}|, |\Omega_{i,max}|)$, with $\Omega_{i,min}$ and $\Omega_{i,max}$ the minimum and maximum bounds on $-\Delta\tau_i/\tau_i$, and $u_{i,min}$ and $u_{i,max}$ the actual saturation levels of vehicle i. We used the fact that $\phi_i = sat(u_i) - a_i$ belongs to $[u_{i,min} - u_{i,max}, u_{i,max} - u_{i,min}]$ by exploiting the properties of a first order system with input sat(u_i) and output a_i. From these bounds we have

$$\begin{aligned} u_{min,m} + \bar{\Omega}(u_{i,min} - u_{i,max}) &\le u_i \\ &\le u_{max,m} + \bar{\Omega}(u_{i,max} - u_{i,min}) \end{aligned} \tag{37}$$

where the result in [25] that $u_{i,bl}$ will converge to $u_{i,m}$ has been used. From (37), one can design $u_{min,m}$ and $u_{max,m}$

$$u_{min,m} \ge \max_i [u_{i,min} - \bar{\Omega}(u_{i,min} - u_{i,max})] \tag{38}$$

$$u_{max,m} \le \min_i [u_{i,max} - \bar{\Omega}(u_{i,max} - u_{i,min})] \tag{39}$$

Remark 6: *In line with [18], [19], the bounds (38)-(39) avoid saturation at the price of reducing performance. To select $\bar{\Omega}$, a bound to the uncertainty $-\Delta\tau_i/\tau_i$ must be known: the more the heterogeneity of the platoon, the tighter $u_{min,m}$ and $u_{max,m}$. If the platoon is homogeneous, (38)-(39) become $u_{min,m} \ge u_{i,min}$ and $u_{max,m} \le u_{i,max}$, i.e. the bounds of the reference model can be the same as the bounds of the vehicles.*

Remark 7: *The bounds in (37) are based on the worst-case uncertainty for Ω_i, and on the worst-case excursion for $\phi_i = sat(u_i) - a_i$. To reduce conservativeness, an efficiency factor can be multiplied to $\bar{\Omega}$ in (37). In simulations, we verified that an efficiency factor of $0.25 \sim 0.5$ reduces conservativeness while still respecting all saturation bounds.*

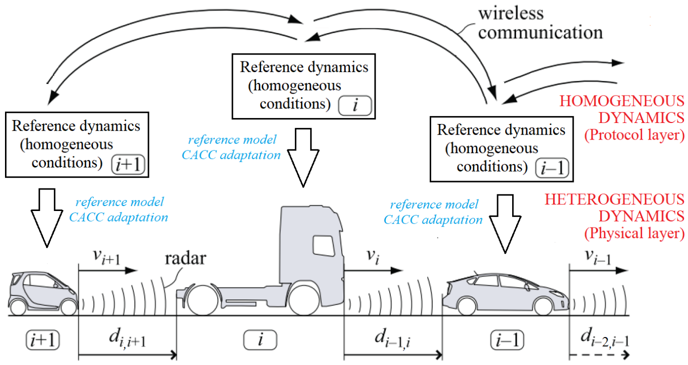

Fig. 2: Homogenization of a heterogeneous platoon.

The dynamics of the vehicle with saturation become

$$\dot{x}_i = A_m^\gamma x_i + B_w w_i + B_u[sat(u_{i,ad}) + \Omega^* \phi_i] \tag{40}$$

and

$$hc_1 \dot{u}_{i,bl} = \begin{cases} -\gamma u_{i,bl} + \xi_{i,bl} & \text{if } u_{i,m} = u_{max,m} \text{ and} \\ & \quad -u_{i,m} + \xi_{i,m} \ge 0 \\ -u_{i,bl} + \xi_{i,bl} & \text{if } u_{min,m} < u_{i,m} < u_{max,m} \\ & \quad \textbf{or } u_{i,m} = u_{max,m} \text{ and} \\ & \quad -u_{i,m} + \xi_{i,m} < 0 \\ & \quad \textbf{or } u_{i,m} = u_{min,m} \text{ and} \\ & \quad -u_{i,m} + \xi_{i,m} > 0 \\ -\gamma u_{i,bl} + \xi_{i,bl} & \text{if } u_{i,m} = u_{min,m} \text{ and} \\ & \quad -u_{i,m} + \xi_{i,m} \le 0 \end{cases} \tag{41}$$

The last equation implies that $u_{i,bl}$ follows a similar law as $u_{i,m}$: furthermore, when $u_{i,bl} \to u_{i,m}$ the two inputs will saturate synchronously. We obtain the dynamics

$$\dot{\tilde{x}}_i = \begin{cases} A_m^\gamma \tilde{x}_i + B_u \tilde{\Omega}_i \phi_i & \text{if } u_{i,m} = u_{max,m} \text{ and} \\ & \quad -u_{i,m} + \xi_{i,m} \ge 0 \\ A_m \tilde{x}_i + B_u \tilde{\Omega}_i \phi_i & \text{if } u_{min,m} < u_{i,m} < u_{max,m} \\ & \quad \textbf{or } u_{i,m} = u_{max,m} \text{ and} \\ & \quad -u_{i,m} + \xi_{i,m} < 0 \\ & \quad \textbf{or } u_{i,m} = u_{min,m} \text{ and} \\ & \quad -u_{i,m} + \xi_{i,m} > 0 \\ A_m^\gamma \tilde{x}_i + B_u \tilde{\Omega}_i \phi_i & \text{if } u_{i,m} = u_{min,m} \text{ and} \\ & \quad -u_{i,m} + \xi_{i,m} \le 0 \end{cases} \tag{42}$$

from which the following stability result can be stated.

Theorem 1: Consider the uncertain system dynamics in (34), and the reference model dynamics in (28) with bounded external reference input w_i. Then for any positive constant Γ_Ω the adaptive input, $\forall i \in S_M$,

$$u_{i,ad} = -\hat{\Omega}_i \phi_i \qquad \dot{\hat{\Omega}}_i = \Gamma_\Omega \phi_i \tilde{x}_i P_m B_u \tag{43}$$

regulates the tracking error asymptotically to zero, i.e. $\lim_{t\to\infty} x_i(t) - x_{i,m}(t) = 0$, $\forall i \in S_M$. In (43) P_m represents a common symmetric positive-definite matrix satisfying

$$A_m^T P_m + P_m A_m < -Q_m \quad (44)$$

$$A_m^{\gamma\,T} P_m + P_m A_m^{\gamma} < -Q_m \quad (45)$$

with $Q_m = Q_m^T > 0$ a design matrix.

Proof. See Appendix A.

Remark 8: From (44) and (45) it can be seen that stability relies on a common Lyapunov function between A_m and A_m^{γ} (i.e. between the unsaturated and saturated dynamics). Such common Lyapunov function allows implies that A_m^{γ} (which can be eventually time-varying) should be close enough to A_m for such a Lyapunov function to exist. This is the case if the formation errors e_i are kept small, which is consistent with the studies [18], [19] (large spacing errors cannot be handled as they cause hitting the saturation bounds).

IV. Simulations

To validate the theoretical analysis, we consider an input-saturated heterogeneous platoon with $M = 5$.

A. Unidirectional vs. Bidirectional string stability

To study string stability, we calculate $|G_{i,r}(j\omega)|$ with $\tau_0 = 0.6$, $h = 0.7$, $k_p = 0.2$ and $k_d = 0.7$ for both the unidirectional ($c_1 = 1$, $c_2 = 0$) and the bidirectional case ($c_1 = c_2 = 0.5$). For the unidirectional case, Fig. 3a shows that the effect of an exogenous disturbance in u_r is attenuated throughout the platoon (being $|G_{i,r}(j\omega)| \le 1$ at each frequency). To show that a bidirectional CACC may not retain string stability unless carefully designed, we consider two possible bidirectional CACC implementations, depending on the weight of the look-ahead error of the last vehicle. In the first implementation, such look-ahead error is weighted as 1 (as in (14)): this results in Fig. 3b. In the second implementation, it is weighted as 0.5 (as the look-ahead errors of the other vehicles), i.e.

$$c_1 h \dot{u}_{M,bl} = -u_{M,bl} + c_1(k_p e_{1,M} + k_d e_{2,M}) + c_1 u_{M-1,bl}.$$

This results in Fig. 3c. Clearly, the second implementation is not beneficial for string stability, as amplifications up to 3% (0.25 dB) occur at low frequencies (<0.2 rad/s) among adjacent vehicles. The first implementation of bidirectional CACC is to be preferred (and it is used in the forthcoming simulations) as it attains analogous string stability properties well known for unidirectional CACC [3]. This validates the effectiveness of the string stability analysis proposed in (11)-(20), whose main benefit is to address in a unified framework both the unidirectional and bidirectional cases: this way, one can easily verify how far (in terms of string stability) a bidirectional CACC is as compared to a unidirectional CACC.

B. Unsaturated vs. Saturated cohesiveness

Having defined homogeneous string stable conditions, let us study the heterogeneous saturated case. To test the algorithms in a realistic setting, in all simulations we consider a communication delay of 0.1s and an engine delay of 0.2s, values in line with CACC literature [5], [6]. Table I presents the platoon's characteristics, with the true values of the uncertainties Ω_i^*, $\forall i \in S_M$, unknown to the designer. However, we assume to know the upper and lower bound of Ω_i^*, be used to design $u_{min,m}$ and $u_{max,m}$. Specifically, $\bar{\Omega} = 0.333$ and the worst case saturation bounds are $u_{min,m} = -1+0.333*2 = -0.333$ and $u_{max,m} = 1 - 0.333 * 2 = 0.333$. After including an efficiency factor of 0.25 as explained in Remark 7, we obtain the bounds -0.83 and 0.83. The adaptive input (43) is designed using (44) with $Q_m = 5I$ and $\Gamma_\Omega = 80$.

TABLE I: Platoon parameters, M=5, h=0.7s

i	0	1	2	3	4	5
$\tau_i(s)$	0.6	0.5	0.7	0.45	0.7	0.8
$u_{min,i}$	-0.83	-1.5	-2.5	-1.0	-2.0	-2.5
$u_{max,i}$	0.83	1.5	2.5	1.0	2.0	2.5
Ω_i^*	0	0.2	-0.143	0.333	-0.143	-0.25

Cohesiveness is tested under acceleration-deceleration phase for the leading vehicle, for three unidirectional scenarios:

- No saturation with baseline (nonadaptive) control, i.e. the standard CACC [3]. This scenario shows cohesiveness in the ideal unconstrained situation;
- Saturation with baseline (nonadaptive) control, to show loss of cohesiveness due to engine constraints;
- Saturation with proposed adaptive control, to show how cohesiveness is recovered by the proposed mechanism.

In view of Remark 1, let us plot the velocity responses as a measure of cohesiveness (regulating the relative velocities close to zero keeps the platoon cohesive), while the inter-vehicle distances (calculated with respect to the preceding vehicle) report whether collisions among vehicles occur. Fig. 4a shows the velocity response in case no saturation is present: all vehicles follow the leader velocity, which implies platoon cohesiveness. Also, the absence of engine constraints lets all vehicles follow the leader acceleration, see Fig. 4b.

In Fig. 5a (saturation with the same baseline control), vehicle 3 is incapable of following the preceding vehicle speed, i.e. cohesiveness is lost. Vehicles 4 and 5 follow vehicle 3 which lost cohesiveness. The triangular shape of the velocity of vehicle 3 results from acceleration/deceleration limits (Fig. 5b), which eventually lead to collision at around 80 seconds.

Fig. 6a results from the proposed CACC: all vehicles maintain cohesiveness. Because of the engine limits, cohesiveness is naturally maintained at the price of reducing performance (the leading vehicle reaches a maximum speed of 30 m/s instead of 44 m/s). This can be clearly seen from Fig. 6b where, as compared to Fig. 4b the high acceleration and deceleration peaks are chopped by the proposed mechanism.

C. Unidirectional vs. Bidirectional cohesiveness

To highlight some limits of unidirectional interaction, an extreme scenario is designed as follows: we take the saturation levels to be the same for all vehicles, i.e. $u_{min,i} = -1$, $u_{max,i} = 1$, resulting in $u_{min,m} = -1$, $u_{max,m} = 1$ (cf. Remark 4). Then, when the platoon is at maximum acceleration, we intentionally provoke vehicle 3 to "slip back" impulsively (this can be imagined as vehicle 3 facing a bump

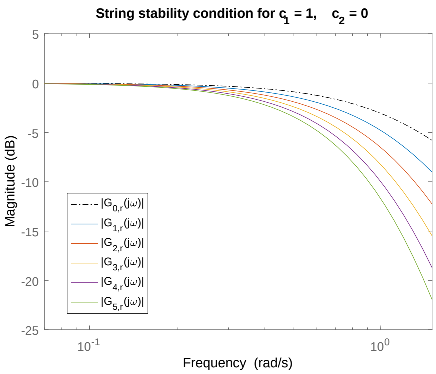

(a) $c_1 = 1$, $c_2 = 0$.

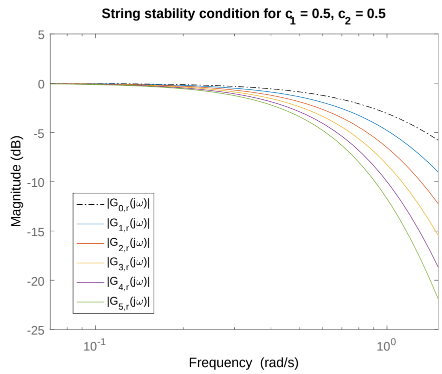

(b) $c_1 = c_2 = 0.5$, and look-ahead error of veh. 5 weighted as 1.

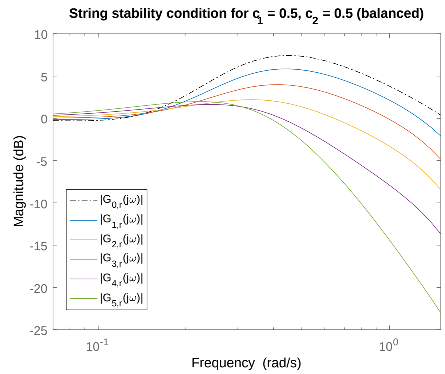

(c) $c_1 = c_2 = 0.5$, and look-ahead error of veh. 5 weighted as 0.5.

Fig. 3: String stability checks for unidirectional and bidirectional cases.

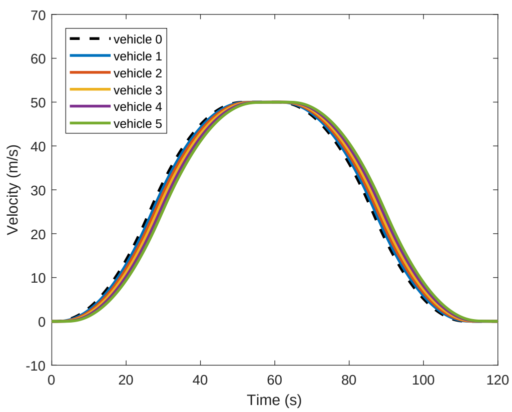

(a) Velocity response.

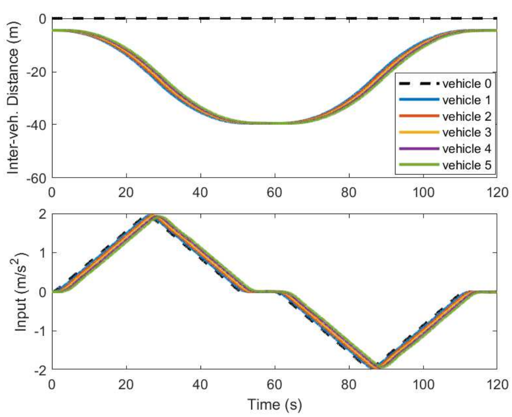

(b) Inter-vehicle distance and unconstrained input.

Fig. 4: No saturation with baseline control.

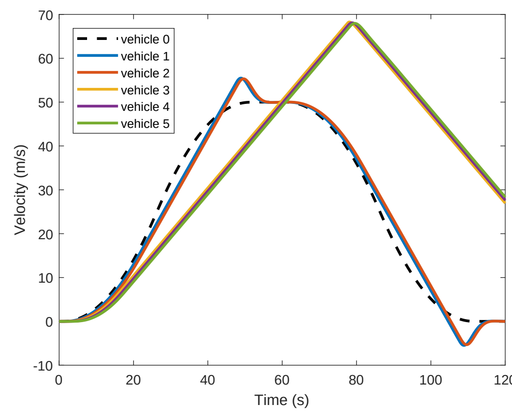

(a) Velocity response.

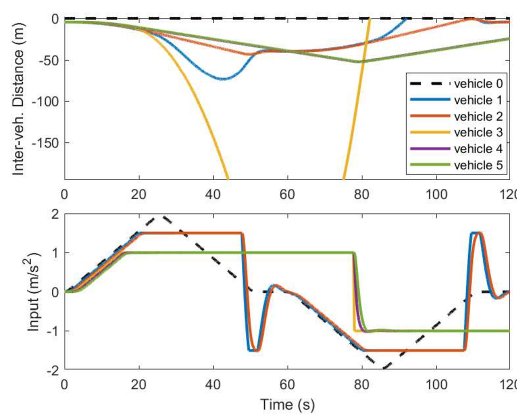

(b) Inter-vehicle distance and constrained input.

Fig. 5: Saturation with baseline control.

or a wet spot on the road): the slip back causes a positive impulse in the distance between vehicle 2 and 3 and a negative impulse in the distance between vehicle 3 and 4. Two scenarios are considered for the proposed adaptive strategy:

- Saturation with unidirectional interaction. This scenario is meant to show that unidirectional control may lose cohesiveness in this extreme case.
- Saturation with bidirectional interaction. This scenario is meant to show that bidirectional control may recover cohesiveness also in this extreme case.

In the unidirectional case, the gap between vehicles 2 and 3 cannot be closed as both vehicles keep maximum acceleration (cf. the positive constant gap in Fig. 7a). In addition, the negative impulse between vehicles 3 and 4 causes vehicle 4

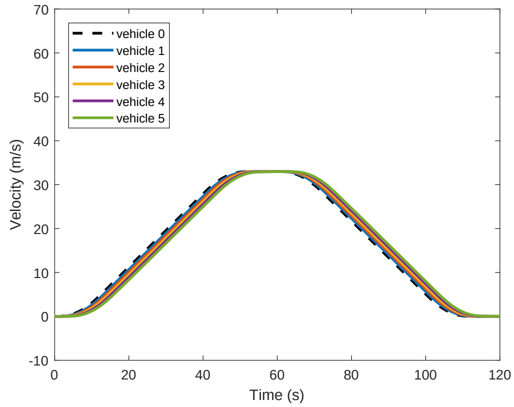

(a) Velocity response.

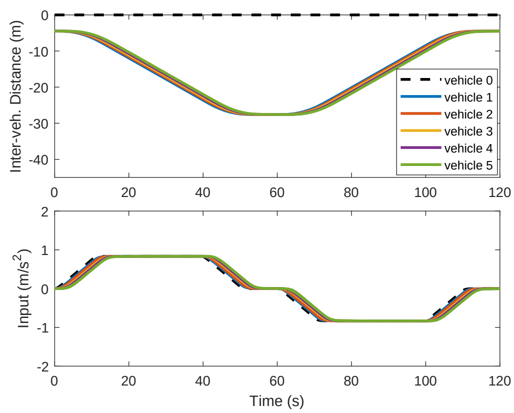

(b) Inter-vehicle distance and constrained input.

Fig. 6: Saturation with proposed control.

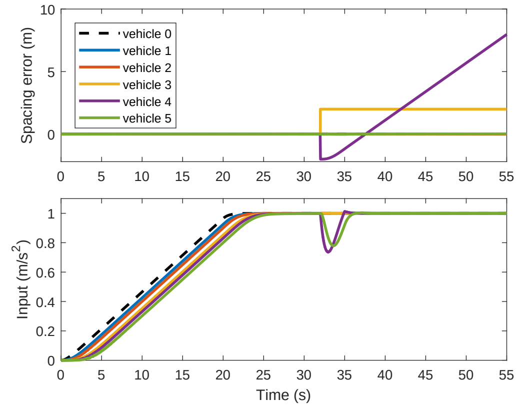

(a) Spacing errors and input responses in unidirectional case.

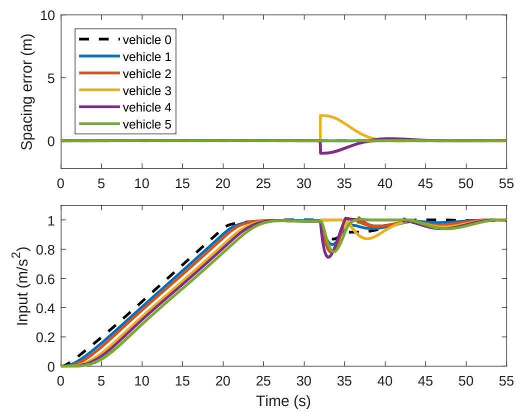

(b) Spacing errors and input responses in bidirectional case.

Fig. 7: Extreme scenario under unidirectional and bidirectional interaction.

to slow down without catching up anymore (cf. the negative impulse in Fig. 7a becoming positive and increasing). In fact, due to unidirectionality, vehicle 3 keeps maximum acceleration despite the gap with vehicle 4, as it only cares about spacing with vehicle 2. Being vehicle 3 at maximum acceleration with higher velocity than vehicle 4, the spacing between vehicles 3 and 4 keeps on increasing.

On the other hand, the gap is closed in Fig. 7b: thanks to bidirectional interaction, vehicles consider both the look-ahead and look-back errors. As a result, vehicle 2 and vehicle 1 can slow down a bit, in order for vehicle 3 to close the gap: then, they can reach maximum acceleration again. Fig. 8a reports the inter-vehicle distances and Fig. 8b reports the distances with respect to the leading vehicle. Fig. 8a shows that bidirectionality leads to shorter inter-vehicle distances, i.e. the platoon is more cohesive (for better readability, only the inter-vehicle distances for vehicles 2, 3 and 4 are reported). Fig. 8b further shows the improved cohesiveness due to bidirectionality. Notice that, in the bidirectional case, the leading vehicle can decelerate a bit to allow vehicle 1 to keep the formation, *even before the disturbance acts on vehicle 3*.

To highlight the effect of communication and engine delays, let us reproduce the simulations of Fig. 7 *without any delay*. The results are in Figs. 9a and 9b in terms of spacing errors and input responses. As compared to the simulations with delays in Figs. 7a and 7b, it can be seen that delays introduce small oscillations when converging to the steady-state input, and slightly longer settling time. It is expected that the presence of delay reduces performance of a controller [40, Sect. 7.4]: yet, the proposed methodology still performs satisfactorily in the presence of such delays.

In the simulations of Figs. 7-9 the leading vehicle always accelerates: this is an extreme scenario designed to test cohesiveness in the most challenging conditions. When the leading vehicle has deceleration phases, it is clear that such phases will help cohesiveness. To this purpose, let us go back to the acceleration-deceleration scenarios of Sect. IV.B, but again intentionally provoking vehicle 3 to ”slip back”. The difference between the unidirectional and bidirectional case can be seen in Fig. 10a and Fig. 10b. Unidirectional interaction creates larger errors: it is only the deceleration phase that helps rejecting the disturbance and prevents loss of cohesiveness. Fig. 10c further highlights that the unidirectional case would lose cohesiveness if the leading vehicle did not decelerate. Again, vehicle 0 decelerates a bit in the bidirectional case to keep the platoon more cohesive, i.e. in Fig. 10c vehicle 1 stays a bit closer to vehicle 0 in the bidirectional case. These simulations highlight the benefits of bidirectional interaction in keeping the formation at all time steps.

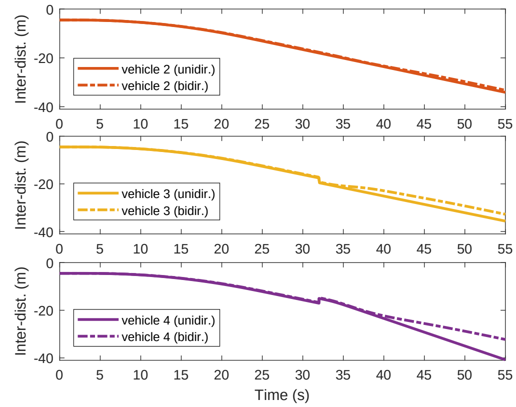

(a) Inter-vehicle distances for vehicles 2, 3 and 4.

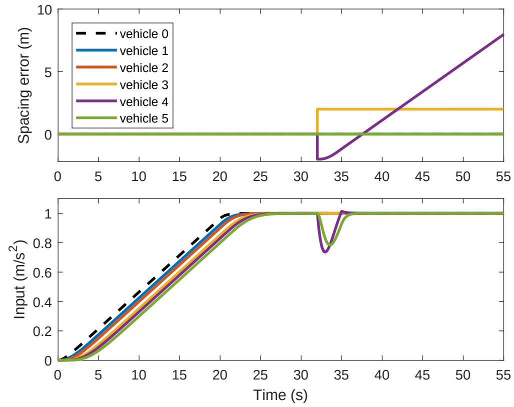

(a) Spacing errors and input responses in unidirectional case.

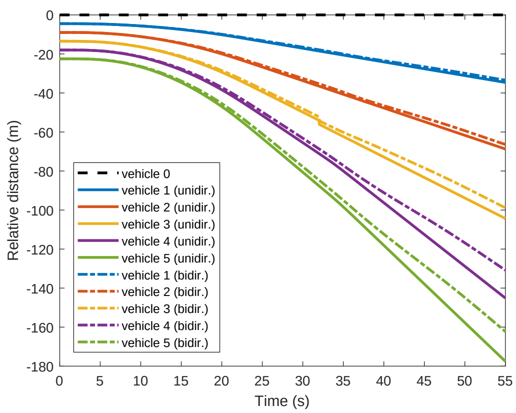

(b) Distances with respect to leading vehicle 0

Fig. 8: Extreme scenarios under unidirectional (solid) and bidirectional (dash-dot) interaction.

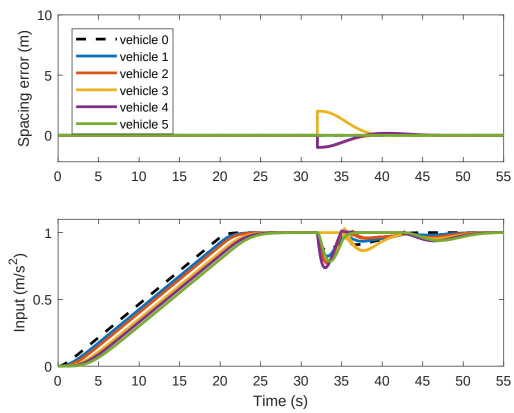

(b) Spacing errors and input responses in bidirectional case.

Fig. 9: Extreme scenarios *without delays* under unidirectional and bidirectional interaction.

V. Conclusions

Adaptive platooning is effective in stabilizing platoons with non-identical and uncertain vehicle dynamics (heterogeneous platoons). In this work we have addressed and solved two aspects usually neglected in adaptive platooning strategies: handling saturation (i.e. engine constraints) in such a way not to lose cohesiveness; handling bidirectional interaction (with front and rear vehicle) in such a way not to lose string stability. We have proposed a mechanism based on making the reference dynamics not too demanding, by applying a properly designed saturation action. The mechanism can retain cohesiveness while handling bidirectional interaction in a string stable way.

In future work, it would be relevant to adaptively learn [41] the best homogeneous dynamics that might lead to the best platooning performance, e.g. induce less engine constraints.

References

[1] H. J. Günther, S. Kleinau, O. Trauer, and L. Wolf, "Platooning at traffic lights," *IEEE Intelligent Vehicles Symposium (IV)*, pp. 1047–1053, 2016.

[2] C. Flores and V. Milanés, "Fractional-order-based ACC/CACC algorithm for improving string stability," *Transportation Research Part C: Emerging Technologies*, vol. 95, pp. 381 – 393, 2018.

[3] J. Ploeg, N. van de Wouw, and H. Nijmeijer, "l_p string stability of cascaded systems: Application to vehicle platooning," *IEEE Transactions on Control Systems Technology*, vol. 22, pp. 786–793, 2014.

[4] M. Hafez, M. Ariffin, M. A. Rahman, and H. Zamzuri, "Effect of leader information broadcasted throughout vehicle platoon in a constant spacing policy," *IEEE International Symposium on Robotics and Intelligent Sensors*, pp. 132–137, 2015.

[5] S. Öncü, J. Ploeg, N. van de Wouw, and H. Nijmeijer, "Cooperative adaptive cruise control: Network-aware analysis of string stability," *IEEE Transactions on Intelligent Transportation Systems*, vol. 15, no. 4, pp. 1527–1537, 2014.

[6] J. Ploeg, E. Semsar-Kazerooni, G. Lijster, N. van de Wouw, and H. Nijmeijer, "Graceful degradation of cooperative adaptive cruise control," *IEEE Transactions on Intelligent Transportation Systems*, vol. 16, no. 1, pp. 488–497, 2015.

[7] A. Firooznia, J. Ploeg, N. van de Wouw, and H. Zwart, "Co-design of controller and communication topology for vehicular platooning," *IEEE Transactions on Intelligent Transportation Systems*, vol. 18, no. 10, pp. 2728–2739, 2017.

[8] U. Montanaro, G. F. M. Tufo, M. di Bernardo, A. Salvi, and S. Santini, "Extended cooperative adaptive cruise control," *IEEE Intelligent Vehicles Symposium (IV)*, pp. 605–610, 2014.

[9] F. Acciani, P. Frasca, A. Stoorvogel, E. Semsar-Kazerooni, and G. Heijenk, "Cooperative adaptive cruise control over unreliable networks: an observer-based approach to increase robustness to packet loss," in *2018 European Control Conference (ECC)*, 2018, pp. 1399–1404.

[10] Y. Li, C. Tang, S. Peeta, and Y. Wang, "Nonlinear consensus-based connected vehicle platoon control incorporating car-following interactions and heterogeneous time delays," *IEEE Transactions on Intelligent Transportation Systems*, vol. 20, no. 6, pp. 2209–2219, 2019.

[11] Y. A. Harfouch, S. Yuan, and S. Baldi, "An adaptive switched control approach to heterogeneous platooning with intervehicle communication losses," *IEEE Transactions on Control of Network Systems*, vol. 5, no. 3, pp. 1434–1444, 2018.

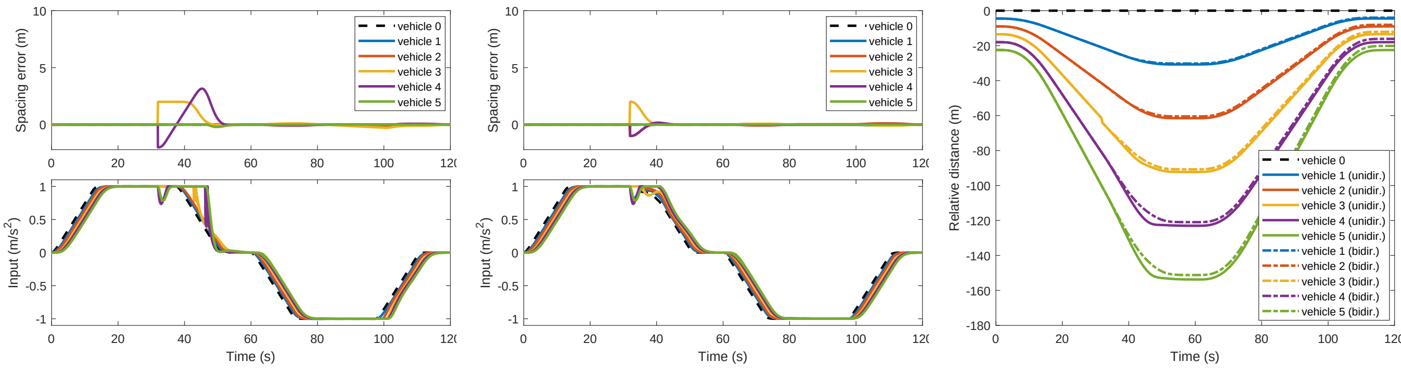

(a) Spacing errors and input responses in unidirectional case.

(b) Spacing errors and input responses in bidirectional case.

(c) Distances from vehicle 0 in unidirectional (solid) and bidirectional (dash-dot) case.

Fig. 10: Additional acceleration-deceleration scenarios under unidirectional and under bidirectional interaction.

[12] V. S. Dolk, J. Ploeg, and W. P. M. H. Heemels, "Event-triggered control for string-stable vehicle platooning," *IEEE Transactions on Intelligent Transportation Systems*, vol. 18, no. 12, pp. 3486–3500, 2017.

[13] M. Di Vaio, G. Fiengo, A. Petrillo, A. Salvi, S. Santini, and M. Tufo, "Cooperative shock waves mitigation in mixed traffic flow environment," *IEEE Transactions on Intelligent Transportation Systems*, pp. 1–15, 2019, doi:10.1109/TITS.2018.2883485.

[14] J. C. Zegers, E. Semsar-Kazerooni, J. Ploeg, N. van de Wouw, and H. Nijmeijer, "Consensus-based bi-directional CACC for vehicular platooning," in *2016 American Control Conference*, 2016, pp. 2578–2584.

[15] M. Nieuwenhuijze, "String stability analysis of bidirectional adaptive cruise control," Master's thesis, Eindhoven University of Technology, The Netherlands, 2010.

[16] M. Pirani, E. Hashemi, J. W. Simpson-Porco, B. Fidan, and A. Khajepour, "Graph theoretic approach to the robustness of k -nearest neighbor vehicle platoons," *IEEE Transactions on Intelligent Transportation Systems*, vol. 18, no. 11, pp. 3218–3224, 2017.

[17] G. Rodonyi, "An adaptive spacing policy guaranteeing string stability in multi-brand ad-hoc platoons," *IEEE Transactions on Intelligent Transportation Systems*, vol. 19, no. 6, pp. 1902–1912, 2018.

[18] S. C. Warnick and A. A. Rodriguez, "Longitudinal control of a platoon of vehicles with multiple saturating nonlinearities," in *Proceedings of 1994 American Control Conference*, vol. 1, 1994, pp. 403–407 vol.1.

[19] M. R. Jovanovic, J. M. Fowler, B. Bamieh, and R. D'Andrea, "On avoiding saturation in the control of vehicular platoons," in *Proceedings of the 2004 American Control Conference*, 2004, pp. 2257–2262 vol.3.

[20] E. Semsar-Kazerooni and K. Khorasani, "Team consensus for a network of unmanned vehicles in presence of actuator faults," *IEEE Transactions on Control Systems Technology*, vol. 18, no. 5, pp. 1155–1161, 2010.

[21] J. C. Zegers, E. Semsar-Kazerooni, J. Ploeg, N. van de Wouw, and H. Nijmeijer, "Consensus control for vehicular platooning with velocity constraints," *IEEE Transactions on Control Systems Technology*, vol. 26, no. 5, pp. 1592–1605, 2018.

[22] W. Gao, F. Rios-Gutierrez, W. Tong, and L. Chen, "Cooperative adaptive cruise control of connected and autonomous vehicles subject to input saturation," in *IEEE 8th Annual Ubiquitous Computing, Electronics and Mobile Communication Conference (UEMCON)*, 2017, pp. 418–423.

[23] S. C. Warnick and A. A. Rodriguez, "A systematic antiwindup strategy and the longitudinal control of a platoon of vehicles with control saturations," *IEEE Transactions on Vehicular Technology*, vol. 49, no. 3, pp. 1006–1016, 2000.

[24] Y. Li, C. Tang, S. Peeta, and Y. Wang, "Integral-sliding-mode braking control for a connected vehicle platoon: Theory and application," *IEEE Trans. on Industrial Electronics*, vol. 66, no. 6, pp. 4618–4628, 2019.

[25] Y. A. Harfouch, S. Yuan, and S. Baldi, "An adaptive approach to cooperative longitudinal platooning of heterogeneous vehicles with communication losses," *20th IFAC World Congress*, pp. 1352 – 1357, 2017.

[26] X. Guo, J. Wang, F. Liao, W. Xiao, and H. Li, "A low-complexity control for nonlinear vehicular platoon with asymmetric actuator saturation," in *2018 IEEE 14th International Conference on Control and Automation (ICCA)*, 2018, pp. 387–392.

[27] X. Guo, J. Wang, F. Liao, and R. S. H. Teo, "CNN-based distributed adaptive control for vehicle-following platoon with input saturation," *IEEE Transactions on Intelligent Transportation Systems*, vol. 19, no. 10, pp. 3121–3132, 2018.

[28] S. Baldi and P. Frasca, "Adaptive synchronization of unknown heterogeneous agents: An adaptive virtual model reference approach," *Journal of the Franklin Institute*, vol. 356, no. 2, pp. 935 – 955, 2019.

[29] S. Baldi, S. Yuan, and P. Frasca, "Output synchronization of unknown heterogeneous agents via distributed model reference adaptation," *IEEE Transactions on Control of Network Systems*, vol. 6, no. 2, pp. 515–525, 2019.

[30] V. Dolk, J. d. Ouden, S. Steeghs, J. G. Devanesan, I. Badshah, A. Sudhakaran, K. Elferink, and D. Chakraborty, "Cooperative automated driving for various traffic scenarios: Experimental validation in the GCDC 2016," *IEEE Transactions on Intelligent Transportation Systems*, vol. 19, no. 4, pp. 1308–1321, 2018.

[31] S. Kokogias, L. Svensson, G. Collares Pereira, R. Oliveira, X. Zhang, X. Song, and J. Mårtensson, "Development of platform-independent system for cooperative automated driving evaluated in GCDC 2016," *IEEE Transactions on Intelligent Transportation Systems*, vol. 19, no. 4, pp. 1277–1289, 2018.

[32] M. Aramrattana, J. Detournay, C. Englund, V. Frimodig, O. U. Jansson, T. Larsson, W. Mostowski, V. D. Rodríguez, T. Rosenstatter, and G. Shahanoor, "Team Halmstad approach to cooperative driving in the Grand Cooperative Driving Challenge 2016," *IEEE Transactions on Intelligent Transportation Systems*, vol. 19, no. 4, pp. 1248–1261, 2018.

[33] O. S. Taş, N. O. Salscheider, F. Poggenhans, S. Wirges, C. Bandera, M. R. Zofka, T. Strauss, J. M. Zöllner, and C. Stiller, "Making Bertha Cooperate–Team AnnieWAY's entry to the 2016 Grand Cooperative Driving Challenge," *IEEE Transactions on Intelligent Transportation Systems*, vol. 19, no. 4, pp. 1262–1276, 2018.

[34] L. Guvenc, I. M. C. Uygan, K. Kahraman, R. Karaahmetoglu, I. Altay, M. Senturk, M. T. Emirler, A. E. Hartavi Karci, B. Aksun Guvenc, E. Altug, M. C. Turan, . S. Tas, E. Bozkurt, . Ozguner, K. Redmill, A. Kurt, and B. Efendioglu, "Cooperative adaptive cruise control implementation of Team Mekar at the Grand Cooperative Driving Challenge," *IEEE Transactions on Intelligent Transportation Systems*, vol. 13, no. 3, pp. 1062–1074, 2012.

[35] I. Parra Alonso, R. Izquierdo Gonzalo, J. Alonso, . García-Morcillo, D. Fernández-Llorca, and M. . Sotelo, "The experience of DRIVERTIVE-DRIVERless cooperaTIve VEhicle-Team in the 2016 GCDC," *IEEE Transactions on Intelligent Transportation Systems*, vol. 19, no. 4, pp. 1322–1334, 2018.

[36] G. J. L. Naus, R. P. A. Vugts, J. Ploeg, M. J. G. van de Molengraft, and M. Steinbuch, "String-stable CACC design and experimental validation: A frequency-domain approach," *IEEE Transactions on Vehicular Technology*, vol. 59, no. 9, pp. 4268–4279, 2010.

[37] Y. Li, C. Tang, K. Li, X. He, S. Peeta, and Y. Wang, "Consensus-based cooperative control for multi-platoon under the connected vehicles environment," *IEEE Transactions on Intelligent Transportation Systems*, vol. 20, no. 6, pp. 2220–2229, 2019.

[38] Y. Li, W. Chen, S. Peeta, and Y. Wang, "Platoon control of connected multi-vehicle systems under v2x communications: Design and experi-

ments," *IEEE Transactions on Intelligent Transportation Systems*, 2019, doi:10.1109/TITS.2019.2905039.
[39] J. Ploeg, D. P. Shukla, N. van de Wouw, and H. Nijmeijer, "Controller synthesis for string stability of vehicle platoons," *IEEE Transactions on Intelligent Transportation Systems*, vol. 15, no. 2, pp. 854–865, 2014.
[40] G. C. Goodwin, S. F. Graebe, and M. E. Salgado, *Control System Design*. Pearson, 2000.
[41] Z. Chen and B. B. Park, "Preceding vehicle identification for cooperative adaptive cruise control platoon forming," *IEEE Transactions on Intelligent Transportation Systems*, pp. 1–13, 2019.

APPENDIX: PROOF OF THEOREM 1

Define a radially unbounded quadratic (and common) Lyapunov candidate function as:

$$V_i(\tilde{x}_i, \Delta\Omega_i) = \tilde{x}_i^T P_m \tilde{x}_i + \tilde{\Omega}_i^2 \Gamma_\Omega^{-1} \tag{46}$$

where $\Gamma_\Omega > 0$ is the gain matrix containing the rates of adaptation, and $P_m = P_m^T > 0$ is a symmetric positive-definite solution to (44). Taking the time derivative of $V_i(\tilde{x}_i, \tilde{\Omega}_i)$ and using the error dynamics in (42) results in:

$$\dot{V}_i(\tilde{x}_i, \Delta\Omega_i) \leq -\tilde{x}_i^T Q_m \tilde{x}_i - 2\tilde{x}_i^T P_m B_u \tilde{\Omega}_i \phi_i + 2(\tilde{\Omega}_i \Gamma_\Omega^{-1} \dot{\tilde{\Omega}}_i)$$

Moreover using the identity $a^T b = b a^T$ results in:

$$\dot{V}_i \leq -\tilde{x}_i^T Q_m \tilde{x}_i + 2(\tilde{\Omega}_i \{\Gamma_\Omega^{-1} \dot{\tilde{\Omega}}_i - \phi_i \tilde{x}_i^T P_m B_u\}) \tag{47}$$

Choosing the adaptive law as in (43) reduces (47) to

$$\dot{V}_i(\tilde{x}_i, \tilde{\Omega}_i) \leq -\tilde{x}_i^T Q_m \tilde{x}_i \leq 0 \tag{48}$$

which proves the uniform ultimate boundedness of $(\tilde{x}_i, \tilde{\Omega}_i)$. Furthermore, it can be concluded from (48) that $\tilde{x}_i \in L_2$. In addition, since w_i is bounded, then $x_{i,m} \in L_\infty$ and consequently, $x_i \in L_\infty$ and $u_{i,bl} \in L_\infty$. Moreover, since Ω_i^* is constant and $\tilde{\Omega}_i$ is bounded, then the estimated value is also bounded, $\hat{\Omega}_i \in L_\infty$. Since $(x_i, u_{i,bl}) \in L_\infty$ and the components of the regressor vector ϕ_i are locally Lipschitz continuous, then the regressor's components are bounded. Therefore, $u_i \in L_\infty$ and $\dot{x}_i \in L_\infty$. Hence, $\dot{\tilde{x}}_i \in L_\infty$, which implies that $\ddot{V}_i \in L_\infty$. Thus, $\dot{V}_i$ is a uniformly continuous function of time. In addition, since V_i has a lower bound, $\dot{V}_i \leq 0$, and $\dot{V}_i$ is uniformly continuous, then by Barbalat's Lemma, V_i tends to a limit, while its derivative tends to zero. Hence, the tracking error $\tilde{x}_i$ tends asymptotically to zero as $t \to \infty$. Because we have used a common Lyapunov function (46) and (44) it is possible to prove that switching to different error dynamics in (42) does not destroy stability [11].

Simone Baldi (M'14-SM'19) received the B.Sc. in electrical engineering, and the M.Sc. and Ph.D. in automatic control engineering from University of Florence, Italy, in 2005, 2007, and 2011. He is currently professor at School of Mathematics, Southeast University, with guest position at Delft Center for Systems and Control, TU Delft, where he was assistant professor in 2014-2019. Since March 2019, he is subject editor of Int. Journal of Adaptive Control and Signal Processing. His research interests are adaptive and learning systems with applications in networked control and intelligent vehicles.

Di Liu received the B.Sc. in information science from Hubei University of Science and Technology, and the M.Sc. in control engineering from Chongqing University of Posts and Telecommunications in 2014 and 2017, respectively. She is now pursuing double PhD degree with School of Cyber Science and Engineering, Southeast University, China, and with Bernoulli Institute for Mathematics, Computer Science and Artificial Intelligence, University of Groningen, The Netherlands. She is recipient of the 2019 Cyber Security Scholarship of China. Her research interests are in control of intelligent traffic and of automated vehicles.

Vishrut Jain received the B.Tech. (Bachelor of Technology) degree in mechanical engineering from VIT University, India in 2017 and is the M.Sc. degree in vehicle engineering from Delft University of Technology, Delft, The Netherlands, in 2019. His research interests include vehicle control and platooning.

Wenwu Yu (M'12-SM'15) received the B.Sc. in information science and M.Sc. in applied mathematics from Southeast University, China, in 2004 and 2007, and the Ph.D. in Electronic Engineering from City University of Hong Kong, China, in 2010. He is the Founding Director of Lab of Cooperative Control of Complex Systems, Deputy Associate Director of Jiangsu Provincial Key Lab of Networked Collective Intelligence, Associate Dean of School of Mathematics, and Full Professor with the Young Endowed Chair Honor in Southeast University, China.

Dr. Yu's research interests include multi-agent systems, complex networks, intelligent transportation systems. Dr. Yu serves as Editorial Board Member of several IEEE journals, including IEEE Trans. on Circuits and Systems II, IEEE Trans. on Industrial Informatics, IEEE Trans. on Systems, Man, and Cybernetics: Systems. He was awarded a National Natural Science Fund for Excellent Young Scholars in 2013, the Ten Thousand Talent Program for Young Top-notch Talents in 2014, and the Cheung Kong Scholars Programme of China for Young Scholars in 2016. Dr. Yu is also the recipient of the Second Prize of State Natural Science Award of China in 2016.